Slipping and Rolling Ratio of Sliding Acceleration for a Water Droplet Sliding on Fluoroalkylsilane Coatings of Different Roughness

Shunsuke Suzuki,[1,2] Akira Nakajima,*[1,2] Munetoshi Sakai,[2] Yuu Sakurada,[1] Naoya Yoshida,[2,3] Ayako Hashimoto,[2] Yoshikazu Kameshima,[1,2] and Kiyoshi Okada[1]

[1]*Department of Metallurgy & Ceramic Science, Tokyo Institute of Technology, 2-12-1 O-okayama, Meguro-ku, Tokyo 152-8552*

[2]*Kanagawa Academy of Science and Technology, 308 East, KSP, 3-2-1 Sakado, Takatsu-ku, Kawasaki 213-0012*

[3]*Center of Collaborative Research, The University of Tokyo, 4-6-1 Komaba, Meguro-ku, Tokyo 153-8904*

(Received October 25, 2007; CL-071184; E-mail: anakajim@ceram.titech.ac.jp)

The effect of surface roughness on the internal fluidity of a water droplet during sliding on an inclined Si surface treated fluoroalkylsilane (FAS) was investigated using particle image velocimetry (PIV). A water droplet slid down by caterpillar-like rotation flow with or without slippage on the solid–liquid interface. The slipping/rolling ratio on the sliding acceleration depended on the surface roughness; the droplet advanced on the rough surface mainly by the rolling mechanism.

Hydrophobic coatings are used for producing water-repellent solid surfaces. The static contact angle has been commonly used for evaluating the static hydrophobicity. For assessing water-shedding kinetics on hydrophobic solid surfaces, recognition of sliding acceleration and velocity characteristics of water droplets has continued to grow.[1]

Recent studies have revealed two components of the water droplets' sliding behavior on the solid surface; caterpillar-like rotation flow (rolling) and slippage at the solid–liquid boundary (slipping).[2,3] The dominant mechanism during sliding depends on the chemical composition and surface state of solids. To date, most such studies have examined a constant velocity region during sliding.

Water droplets commonly accelerate during the early stage of sliding.[4] This motion often appears over the entire evaluation range. However, few studies have examined the change of the sliding acceleration ratio between rolling and slipping components during sliding.[5] The effect of the surface state on this ratio is not reported, probably because of the difficulties associated with the evaluation of sliding acceleration of these two components during practical sliding.

Very recently, we developed a new particle image velocimetry (PIV) system for direct observation of the internal fluidity of a water droplet during sliding.[6] For the present study, we treated a Si surface with fluoroalkylsilane and prepared hydrophobic coatings with different roughnesses. These two components' sliding acceleration was then evaluated using our PIV system, with specific attention to the internal fluidity of the sliding water droplets.

A Si plate ((100), $15 \times 40\,mm^2$) was precleaned by irradiation of vacuum UV light. For this study, 1*H*,1*H*,2*H*,2*H*-perfluorodecyltrimethoxysilane (FAS17, $CF_3(CF_2)_7(CH_2)_2Si(OCH_3)_3$) was employed as the hydrophobic agent. Smooth FAS17 coatings were prepared by chemical vapor deposition (CVD). The Si plate was heated with 0.02 mL of FAS17 (TSL8233; GE Toshiba Silicones, Tokyo, Japan) in a Petri dish by flowing N_2 at 150 °C for 1 h. Then, the surface was rinsed and dried (sample A). Rough FAS17 coatings were prepared by soaking method. The FAS17 was dissolved into pure xylene (as prepared; Wako Pure Chemical Industries Ltd., Osaka, Japan) or water-saturated xylene. The FAS17 concentration was adjusted to 25 mM. The cleaned Si plates were soaked into these solutions (100 mL, each) for 70 h at room temperature, then rinsed, and dried (sample B; prepared from pure xylene, sample C; prepared from the water-saturated xylene).

Surface roughness was evaluated in 5-μm^2 area using atomic force microscopy (AFM) with a Si cantilever. Static contact angles of 4-μL water droplets were measured with a contact angle meter (Dropmaster 500; Kyowa Interface Science Co., Ltd., Saitama, Japan) using sessile drop method. The sliding angle (SA) and advancing and receding contact angles were evaluated for 30-μL water droplets using an automatic measurement system (SA-20; Kyowa Interface Science). The PIV analysis was performed for a 35-μL water droplet with 0.06 mass % fluorescent particles (R0300; Duke Scientific Corp., CA, USA) on the sample surface tilted at 35°. Sequential images of the droplet were taken using a high-speed camera. A sheet-shaped Ar laser beam was inserted vertically into the center of the droplet as a light source. The graphical abstract includes a schematic illustration of this system; details were also described in ref 6. For this study, we set a meshed cell image with ca. 125 μm^2 and the time separation of 0.33 ms for sample A, and 20 ms for samples B and C. The velocity vectors were evaluated using commercial software (DIP-Flow; Ditect Inc., Tokyo, Japan) for PIV pattern matching using the correlation factor of 0.60 or greater.

Figures 1a–1c show AFM images of samples A, B, and C. The respective surface roughness values (*R*a) for these samples were 0.20, 3.1, and 13 nm. The coatings from xylene-based solutions exhibited greater roughness than that from CVD. In the xylene solution, dehydration and self-condensation of FAS17 molecules advance. Their rate increases by adding water to the solution.[7]

Table 1 shows values of *R*a, static water contact angle (θ_s), SA, and advancing and receding contact angles at SA (θ_A and θ_R) obtained for each sample. With the increasing *R*a value,

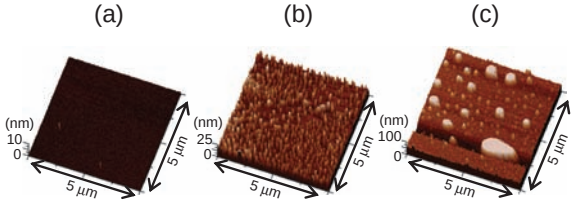

Figure 1. AFM images of the sample surfaces.

Table 1. Surface roughness and static and dynamic angles of water droplet on the sample surfaces

Sample	*R*a/nm	θ_s/deg	SA/deg	θ_A/deg	θ_R/deg
A	0.20	108 ± 1	11 ± 1	120 ± 2	104 ± 1
B	3.1	113 ± 1	15 ± 1	123 ± 1	97 ± 8
C	13	117 ± 1	21 ± 1	128 ± 3	97 ± 2

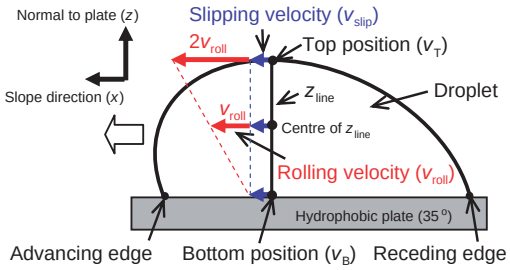

Figure 2. Modeling of the droplet's internal fluidity.

the θ_s and θ_A increased, whereas the θ_R decreased, implying that the contact angle hysteresis (CAH; the difference between θ_A and θ_R) increased as the surface became rougher. We have revealed that small hydrophilic areas exist in the surface of the silane clusters.[7] Consequently, surface roughness in the coatings of this study should include the chemical heterogeneity, which should also increase the CAH and SA by pinning the receding contact line.

As described previously,[6] the outer circumference of the droplet had larger velocity vectors than the droplet interior during sliding. Moreover, shape deformation during sliding was almost negligible in this measurement. Figure 2 presents a schematic diagram of the conceptual model of the internal fluidity for the droplet descending on the inclined plane. The z_{line} is described vertically for the z axis passing the top and the bottom positions. Using this model and PIV analysis, the slipping velocity (v_{slip}) and the rolling velocity (v_{roll}) for slope direction (x) of the droplet can be evaluated experimentally as eqs 1 and 2.[6]

$$v_{slip} = v_B \quad (1)$$

$$v_{roll} = (v_T - v_B)/2 \quad (2)$$

Herein, v_B and v_T are the internal flow velocities evaluated from PIV analysis at the bottom and top positions.

For all observed water droplets, the flow velocity for the x direction (v_x) increased linearly with z height along with z_{line}.[9] Furthermore, the actual sliding velocity measured from the sliding distance at the advancing edge (v_{AD}) coincided with evaluated values using the v_{roll} and v_{slip} as $v_{AD} = v_{roll} + v_{slip}$.[9] These results suggest that the modeling and evaluation of each velocity were appropriate and that effects of surface curvature of droplets and scattering or reflection of emitted light are almost negligible as was confirmed in the previous study.[6] Figure 3 shows the v_{slip} and v_{roll} components evaluated from the PIV analysis for a 35-μL water droplet sliding on these sample surfaces against time. The inset-plot in Figure 3 shows a magnified image of the plots for samples B and C. The v_{slip} is larger than v_{roll} on the smooth surface (sample A). Moreover, they increased with a large slope; large acceleration. On the rough surfaces (samples B and C), v_{slip} and v_{roll} decreased remarkably. No

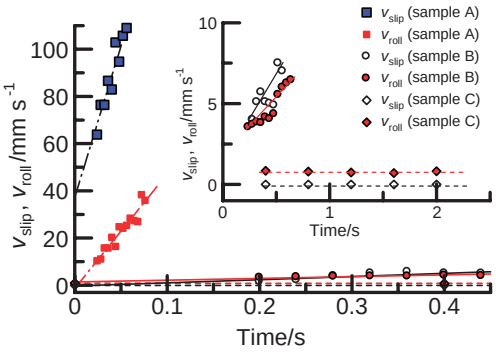

Figure 3. v_{slip} and v_{roll} against time for each sample.

v_{slip} was observed for sample C, implying that a water droplet slid down only by rolling mechanism with a small constant velocity. The actual sliding acceleration values of the advancing edge (a_{AD}) were 1.5 ± 0.1, 0.05 ± 0.05, and ca. 0 m s^{-2} for samples A, B, and C, respectively. The each of a_{AD} was almost equal to the sum of the slipping and rolling acceleration (a_{slip} and a_{roll}) obtained from the slope of the v_{slip} and v_{roll} in Figure 3. We calculated the slipping/rolling ratio ($R = a_{slip}/a_{roll}$) as ca. 2.9 and ca. 2.0 for samples A and B, suggesting that this ratio depended on the surface roughness. The surface roughness with the magnitude of nanometer-scale is known to affect the slippage of the flow on the solid–liquid interface.[8] For the droplet's sliding on the rough surface, the rolling mechanism is advantageous to avoid the large friction drag by slippage at the water–solid interface.

Consequently, the surface roughness had different contributions to slipping and rolling motions of the droplets. The greater slipping motion on the solid–liquid interface might play an important role in the droplet's sliding with large velocities and acceleration on inclined hydrophobic surfaces. Separating the effects of physical surface roughness from chemical heterogeneity on the slipping/rolling ratio of sliding acceleration will be addressed in future studies.

We thanks to JSPS Research Fellow (H17-08586).

References and Notes

1 A. Nakajima, *J. Ceram. Soc. Jpn.* **2004**, *112*, 533.
2 S. Gogte, P. Vorobieff, R. Truesdell, A. Mammoli, F. van Swol, P. Shah, C. J. Brinker, *Phys. Fluids* **2005**, *17*, 51701.
3 M. Sakai, J.-H. Song, N. Yoshida, S. Suzuki, Y. Kameshima, A. Nakajima, *Langmuir* **2006**, *22*, 4906.
4 T. Podgorski, J.-M. Flesselles, L. Limat, *Phys. Rev. Lett.* **2001**, *87*, 036102.
5 A. Nakajima, S. Suzuki, Y. Kameshima, N. Yoshida, T. Watanabe, K. Okada, *Chem. Lett.* **2003**, *32*, 1148.
6 M. Sakai, A. Hashimoto, N. Yoshida, S. Suzuki, Y. Kameshima, A. Nakajima, *Rev. Sci. Instrum.* **2007**, *78*, 045103.
7 S. Suzuki, A. Nakajima, N. Yoshida, M. Sakai, A. Hashimoto, Y. Kameshima, K. Okada, *Langmuir* **2007**, *23*, 8674.
8 E. Lauga, M. P. Brenner, H. A. Stone, in *Handbook of Experimental Fluid Dynamics*, ed. by J. Foss, C. Tropea, A. Yarin, Springer, New York, **2005**, Chap. 15, Sect. 5.1, p. 11.
9 Supporting Information is available electronically on the CSJ-Journal Web site, http://www.csj.jp/journals/chem-lett/index.html.

Published on the web (Advance View) December 8, 2007; doi:10.1246/cl.2008.58